International Journal of Coal Geology 200 (2018) 166–172

Contents lists available at ScienceDirect

International Journal of Coal Geology

journal homepage: www.elsevier.com/locate/coal

Strengthening mylonitized soft-coal reservoirs by microbial mineralization

Chenpeng Song[a,b,*], Derek Elsworth[b]

[a] National and Local Joint Engineering Laboratory of Traffic Civil Engineering Materials, Chongqing Jiaotong University, Chongqing 400074, China
[b] Department of Energy and Mineral Engineering, EMS Energy Institute and G3 Center, Pennsylvania State University, University Park, PA 16802, USA

ARTICLE INFO

Keywords:
Microbial mineralization
Mylonitized soft-coal
Hydraulic fracturing
Microbial cementation

ABSTRACT

Mylonitized-soft-coal is common throughout central China and results from the crushing of intact coal into fine particles under extreme tectonic stress. The fine particles result in very low permeability and hydraulic fracturing to recover natural gas is difficult due to the very low mechanical strength. Enhancing structural integrity and mechanical strength of these coals are the keys to efficiently extracting coalbed methane (CBM). The following explores using microbially-induced calcium carbonate cementation to strengthen and stiffen the coal – and therefore enable successful hydraulic fracturing. We explore the impact of this cementation on the mechanical properties and on microscopic mechanisms of failure for granular assemblages of four sizes. Results indicate significant strength gain after only short periods of biochemical reaction (hours to days) with four cycles of microbial injection (~2 days) yielding a maximum compressive strength (UCS) of ~12 MPa and a brittleness index of 0.17 exceeding that of hard coal. Notably, a higher calcium carbonate content does not automatically guarantee a higher strength- indicating that the distribution of the mineralization and the quality of the particle-particle bonding exerts key control. Also, for identical injection volumes, the resulting calcium carbonate content differs significantly with particle size – larger particle size samples can accommodate larger masses of calcium carbonate. Imaging by SEM indicates that precipitation first occurs on the particle surface, partially enveloping it, before creating particle-particle bonds – thus maintaining grain-pore and pore-pore fluid transport connectivity. As the void is occupied, the cementation process slows, halts, as bacteria and nutrient are expended, and further supply is limited. Therefore, for a fixed duration of supply, the interparticle space of the smaller particle-size will be the first to be bonded and the carbonate content of the smaller particle-size samples will be lower than that for larger particles.

1. Introduction

Coal bed methane (CBM) has become an important source of energy in China, due to its abundance. China is reported to have a resource of 36.8 trillion m^3, ranking it third worldwide (Wang et al., 2017a; Wang et al., 2017b). Hydraulic fracturing is typically used to increase productivity in the usually low-permeability CBM reservoirs. Chinese CBM reservoirs are particularly difficult to produce since they have undergone high levels of tectonic distortion (mylonitized coal) – leaving the coal weak, difficult to hydraulically fracture and consequently with very low permeability. Such mylonitized coal has been tectonically crushed into fine particles then re-compacted. Individual particles are generally < 1 mm in diameter with such seams accounting for 53% of the total coal seams and ~39% of the CBM reserves (Chun, 2014).

CBM extraction rates and cumulative mass recovered may be increased in hard coal through hydraulic fracturing – this is feasible due to the higher mechanical strength, greater structural integrity and resulting greater reach and higher conductivity of the fluid-driven fracture (Zhang et al., 2014; Zou et al., 2011). But for mylonitized soft-coal, due to its granular nature and very low mechanical strength, hydraulic fracturing is difficult. Even if successful in creating a distinct hydraulic fracture, fracture diagenesis and loss of function may result from the clogging with small coal particles and as a result of proppant embedment – resulting in little long-term improvement in permeability. Hence, enhancing the mechanical strength and structural integrity of mylonitized soft coal is an important scientific and technical issue capable of significantly increasing CBM output by enabling the potential success of hydraulic fracturing.

One such method to increase the integrity of fractured coal seams and to enable routine hydraulic fracturing is via microbial cementation. Progress in microbial metallogenia shows that certain strains of microorganisms (Achal et al., 2011; Bang et al., 2001) can rapidly secrete

* Corresponding author at: National and Local Joint Engineering Laboratory of Traffic Civil Engineering Materials, Chongqing Jiaotong University, Chongqing 400074, China.
E-mail address: songchenpeng@163.com (C. Song).

https://doi.org/10.1016/j.coal.2018.11.006
Received 9 June 2018; Received in revised form 7 November 2018; Accepted 7 November 2018
Available online 09 November 2018
0166-5162/

calcium carbonate ($CaCO_3$) by utilizing urea and calcium ions. This form of microbially produced calcium carbonate has a high mechanical strength, is able to act as a cement with the process fundamentally different from chemosynthesis.

The following explores the possibility of using microbial cements to strengthen and stiffen coal – and therefore enable successful hydraulic fracturing. We explore the impact of this cementation on the ensemble mechanical properties and micromechanical behavior of microbially-induced calcium carbonate cementation in mylonitized soft-coal.

2. Overview of microbially-induced mineralization

This study uses Sporosarcina Pasteurii as the microbial stock for the cementation of coal. Sporosarcina Pasteurii is a non-pathogenic nitrogen-circulating bacterium and can maintain strong biological activity in certain harsh environments – including those of high acidic or basic conditions and under high salinity (Kaltwasser et al., 1972). The bacterium can continually produce highly active urease as a result of its own metabolic process. Urease has two major roles in nature: one is in transforming both organismal and external urea into a nitrogen source, and the second is in forming the ammonia nitrogen transport route (Mobley and Hausinger, 1989; Benini et al., 1999). Urease can catalyze the hydrolysis of urea, increasing the rate of hydrolysis by a factor of 10,000, to produce ammonia and carbon dioxide. These products then diffuse into solution through the cell wall and rapidly hydrolyze to NH_4^+ and CO_3^{2-} (Jabri et al., 1995). If calcium ions are present in the solution then they are adsorbed onto the bacterial cell surface due to its negative charge. The carbonate generated from the hydrolysis then forms calcium carbonate precipitate which then envelops the bacterium (Dejong et al., 2006). Simultaneously, ammonium ions generated by the decomposition of urea in the culture solution transform the environment near the microbial cells to alkaline and also contribute to the precipitation of calcium carbonate. The bacteria provide urease and also act as nucleation sites for the calcium carbonate. The process of Sporosarcina Pasteurii induced calcium carbonate production is shown at Fig. 1 (Dejong et al., 2010).

3. Experiments on microbial mineralization in mylonitized soft-coals

We report experiments to culture Sporosarcina Pasteurii with appropriate nutrient solutions in mylonitized soft-coal and to measure resulting changes in stiffness, strength and brittleness. Changes in strength are measured and mechanisms of deformation examined using SEM.

Table 1
Ingredients of ammonium-yeast extract medium ATCC 1376.

Constituents	Concentration
Yeast extract	20.0 g
$(NH_4)_2SO_4$	10.0 g
0.13 M Tris buffer(PH 9.0)	1.0 L
Agar	20.0 g

3.1. Microbial stock and growth conditions

Sporosarcina Pasteurii is utilized as the cultured microbial stock as obtained from the American Type Culture Collection (ATCC 118591, lyophilized powder). The culture medium is NH4-YE (ATCC 13760). The solution is cultured for 24 h at 30 °C, reaching the late exponential/early stationary phase of evolution. The bacteria are stored, suspended in their growth medium, at 4 °C prior to use with measurements of optical density used as an indication of biomass concentration. Optical density is measured using a spectrophotometer at a wavelength of 600 nm. Biomass concentration (Y) is recovered from the optical density (OD_{600}) as $Y = 8.59x10^7 OD_{600}^{1.3627}$, where Y is biomass concentration per ml and OD_{600} is the optical density at a wavelength of 600 nm (Paassen, 2009). Samples are diluted to yield uniform concentrations of $OD_{600} = 1.6$ (Table 1).

3.2. Mylonitized coal samples

Mylonitized coal samples are obtained as block samples from the Moxinpo coal mine near Chongqing, China. As sampled, this coal has a natural particle size of < 1 mm. We sieve to remove the > 20 mesh size (0.85 mm) particles and divide the sub-20 mesh size into four categories: 20–40 mesh (0.85 mm–0.425 mm), 40–60 mesh (0.425 mm-0.250 mm), 60–80 mesh (0.250 mm–0.180 mm), and full-grade mesh (< 0.85 mm) sizes. The individual particles of the mylonitized soft-coal are generally < 1 mm in diameter. Therefore, the samples from the full-grade mesh can be regarded as the real samples. Right cylindrical samples are reconstituted by pressing in a mold at 5 *MPa* for 10 mins so that the structure of the coal is close to the in situ behavior. These samples are then introduced into a flow-through system for

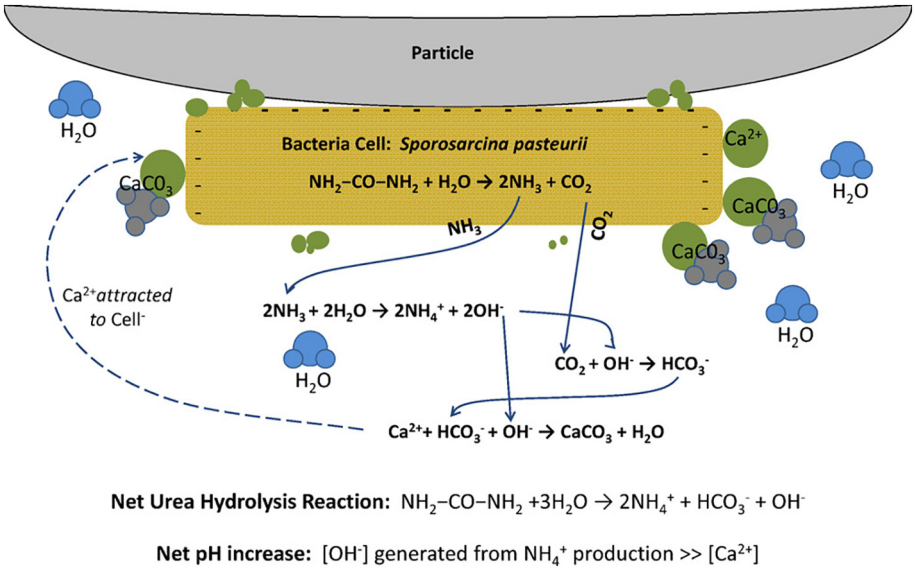

Fig. 1. Principal mechanisms for the formation of calcium carbonate by Sporosarcina Pasteurii (Dejong et al., 2010).

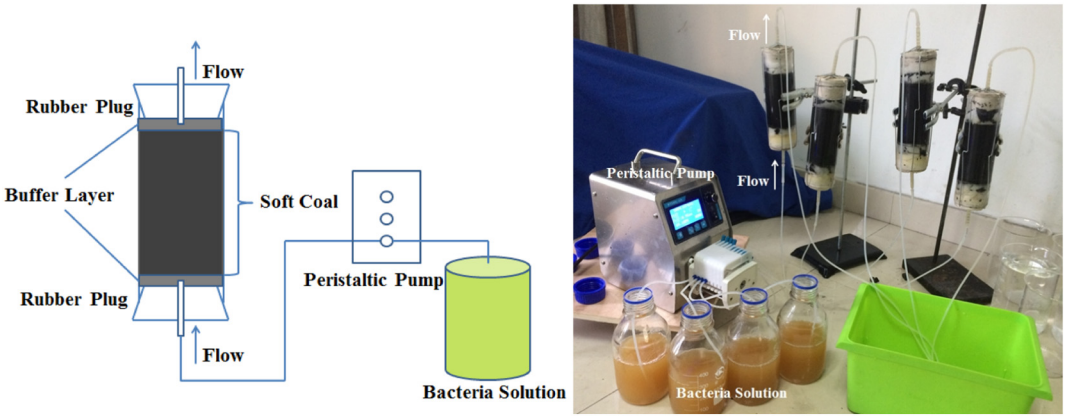

Fig. 2. Schematic of experimental facility.

Fig. 3. Samples after completion of the bacterial injection procedure.

mineralization. Although the coal particles are reconstituted by compaction, no water nor binder are added during do not have any significant initial strength (cohesion).

3.3. Experimental facility and procedure

The experimental facility is shown in Fig. 2. A cylindrical acrylic tube (50 mm diameter and 200 mm length) capped top and bottom with flow-through rubber plugs is used as the experimental core holder. The sample has a permeable buffer layer at fluid inlet and outlet with the coal samples present between. The buffer layer uniformly distributes flow across the full cross-sectional area of the coal sample. Nutrient solution is supplied from a reservoir via peristaltic pump connected to the basal inlet of the core holder.

Cementation is accomplished by staged introduction of bacteria, stabilizing fluid and the nutrient solution into the sample. The standardized test procedure is as follows:

a) Ultrapure water is injected into the sample from the base to fully remove air and to saturate the sample.
b) The bacterial liquid is injected into the sample at the rate of 5 mL/min to fill a single pore-volume of the sample and until it exits the top of the sample.
c) The sample stands for 2 h for the bacteria to be adsorbed to the surface of the coal particles.
d) Stabilizing solution is injected into the sample at 5 *mL*/min for 30 min. We use 0.05 *mol/L* calcium chloride solution for the chloride ions to neutralize the negative charge on the surface of the bacteria. This enables the bacteria to affix more securely to the surface of the negatively charged coal particles and to prevent their subsequent removal when the nutrient solution is later injected. The nutrient (cementing) fluid is injected at 0.5 *mL*/min for 4.0 h. This solution comprises 1.0 *mol/L* calcium chloride and 1.0 *mol/L* carbamide.
e) Upon completing procedures b-d, flow through the sample is reversed across the sample (turned through 180° so that the inlet is now the outlet) and the procedure repeated. One repeat of the end-on-end procedure constitutes a single full injection schedule/cycle.

The four categories of coal samples are individually exposed to 2, 3 and 4 cycles of bacterial injection to represent different durations of exposure.

After the injection procedure is completed, the coal samples are dried for 24 h and trimmed into standard samples for uniaxial compression experiments [Fig. 3].

3.4. Uniaxial compressive strength (UCS) and brittleness of samples

We measure the pre- and post-peak strength response together with the peak strength and brittleness. The stress-strain curves for the mineralized coal samples are shown in Fig. 4 and peak strengths documented in Table 2. Overall, peak strength increases with an increase in the bacterial injection volume. After 4 cycles of injection, the maximum unconfined compressive strength (UCS) of all individual samples is 11.9 MPa for the 40–60 mesh sample. However, coal samples with different particle sizes at different injection volumes exhibit significant differences in the stress-strain curve characteristics. Therefore, knowledge of UCS alone is insufficient to define whether the coal sample is suitable for hydraulic fracturing after microbial cementation. Brittleness is used to identify the possible failure characteristics of the rock mass. For hydraulic fracturing, the possibility of creating an effective fracture is related to many factors, among which the brittleness of the reservoir plays a significant role (Zhang et al., 2016; Hucka and Das,

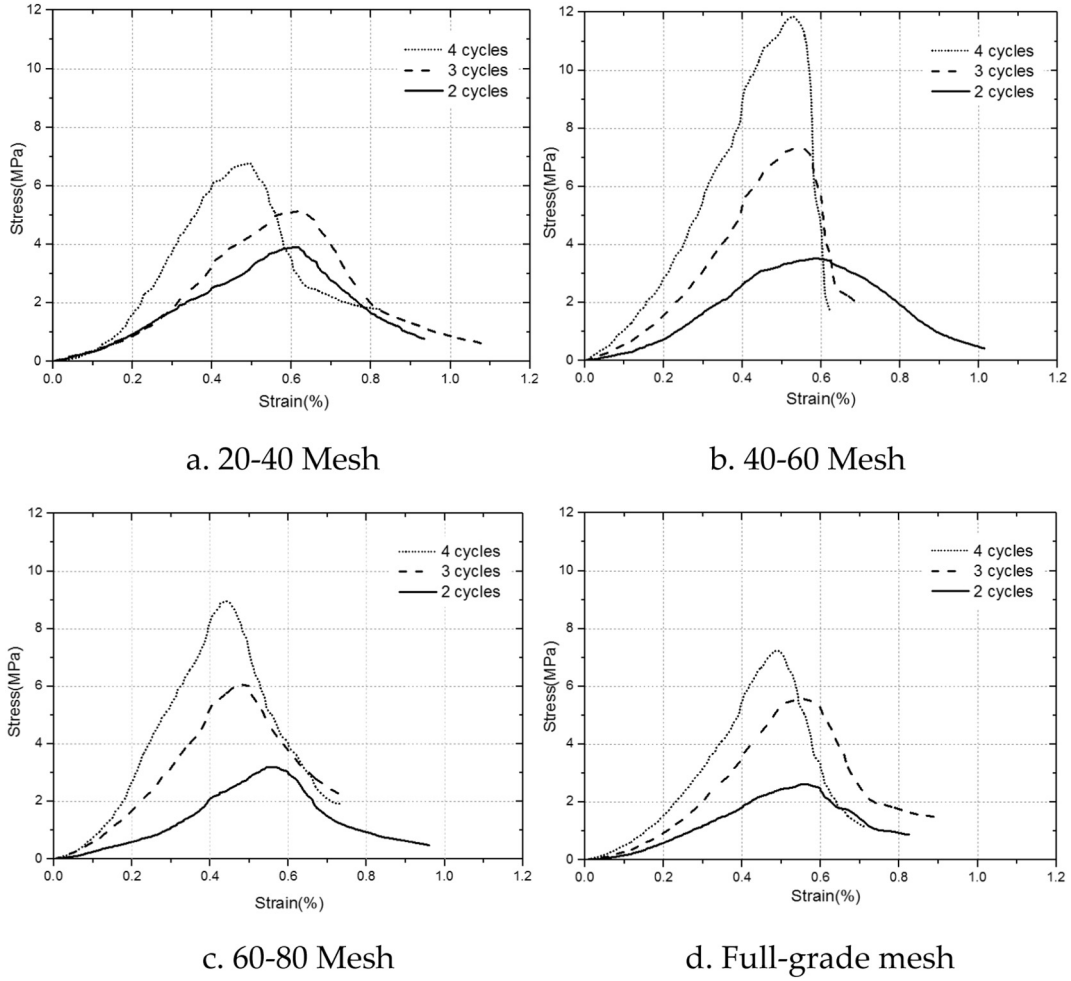

Fig. 4. Stress-strain curves of coal samples after microbial mineralization.

Table 2
The uniaxial compressive strength (UCS) of coal samples.

Injection times	2 cycles	3 cycles	4 cycles
Categories			
20–40 mesh	3.92 MPa	5.13 MPa	6.77 MPa
40–60 mesh	3.52 MPa	7.32 MPa	11.91 MPa
60–80 mesh	3.20 MPa	6.12 MPa	9.02 MPa
Full-grade mesh	2.63 MPa	5.56 MPa	7.23 MPa

Table 3
The brittleness index of coal samples.

Injection times	2 cycles	3 cycles	4 cycles
Categories			
20–40 mesh	0.0675	0.0831	0.0918
40–60 mesh	0.0698	0.1131	0.1691
60–80 mesh	0.0710	0.0758	0.1098
Full-grade mesh	0.0558	0.0817	0.1179

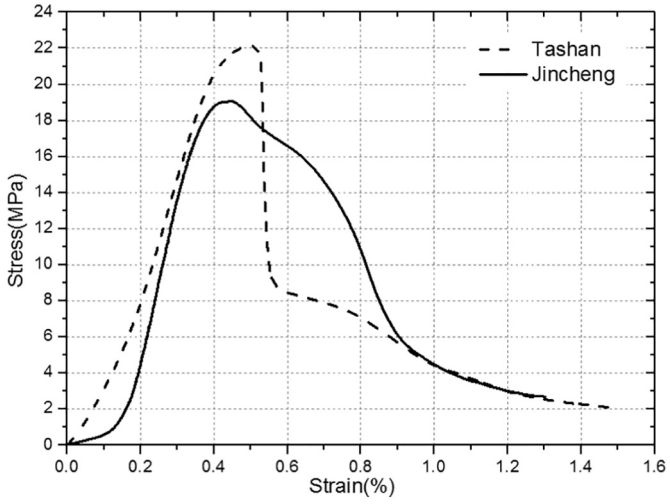

Fig. 5. Stress-strain curves of coal samples from the Tashan mine and the Jincheng coalfield.

1974). Although nearly twenty indicators of rock brittleness (based on strength, stress-strain curve, loading and unloading test, hardness, mineral compositional analysis, etc.) have been proposed (Hajiabdolmajid and Kaiser, 2002; *Brittleness index[M]*, 2014; Xia et al., 2017), the post-peak stress-strain curve is a straightforward and robust approach for its rapid determination. A steep post-peak strength drop characterizes high brittleness, thus it is defined by the relative magnitude and absolute rate of post-peak stress drop.

The brittleness index(BI) is defined as (Meng et al., 2015),

$$BI = \frac{\tau_p - \tau_r}{\tau_p} \frac{\lg |k|}{10}$$

Table 4
The brittleness index of coal samples from the Tashan mine and the Jincheng coalfield.

Coal sample	Brittleness index
Tashan	0.1423
Jincheng	0.1080

Table 5
The $CaCO_3$ mass percent of coal samples.

Injection times	2 cycles	3 cycles	4 cycles
Categories			
20–40 mesh	3.02%	5.85%	7.74%
40–60 mesh	3.18%	4.12%	5.83%
60–80 mesh	3.02%	3.93%	4.72%
Full-grade mesh	3.31%	4.39%	5.76%

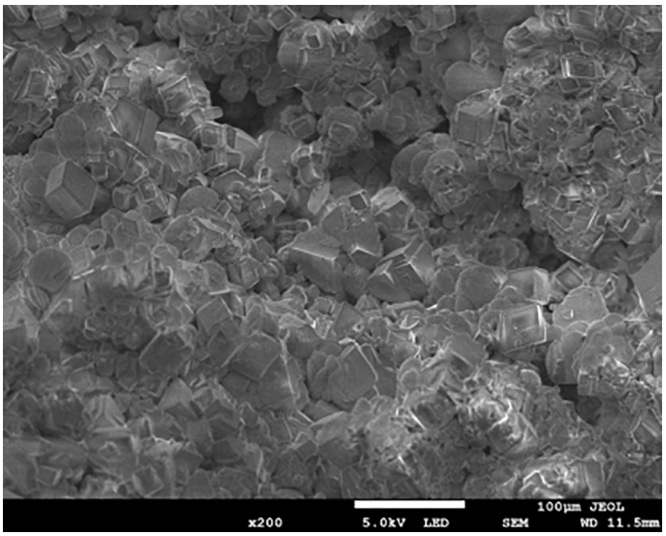

Fig. 6. Crystals of calcium carbonate.

where τ_p is peak strength of UCS, τ_r is residual strength, and $k$is the slope of the stress-strain curve from the point of peak strength to the point of residual strength.

This yields the brittleness index of the coal samples tested here, as shown in Table 3. For comparison, we performed UCS tests and

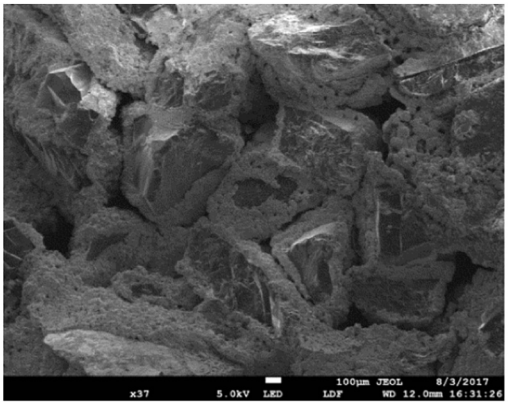

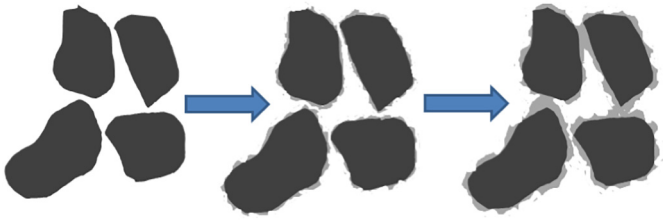

Fig. 8. The cementation process for calcium carbonate via interparticle bonding. Precipitation occurs first on the particle surface, partially enveloping them, before creating particle-particle bonds.

calculated brittleness index for hard coal that is suitable for hydraulic fracturing from the Tashan coal mine and the Jincheng coalfield in China (Fig. 5 and Table 4).

The UCS of the coal samples from both the Tashan mine and Jincheng coalfield are all-greater than those that are microbially-treated and cemented. However, the brittleness index of the coal samples after four cycles of injection typically approaches and sometimes even exceeds that of the coal samples of the hard coal. The maximum BI value (40–60 mesh sample) reaches 0.17, implying the suitability of the treated sample for successful hydraulic fracturing, based on brittleness.

Post failure, the calcium carbonate content of the samples is measured by immersing a part of each sample into *1.0 mol/L* hydrochloric acid and then measuring the mass of $CaCO_3$ produced (Table 5).

Calcium carbonate content increases with an increase in the bacterial injection volume – potentially linking the impact of increased carbonate content to stronger cementation. However, significant differences exist among the UCS magnitudes for different particle sizes and with measured concentrations of calcium carbonate content. After

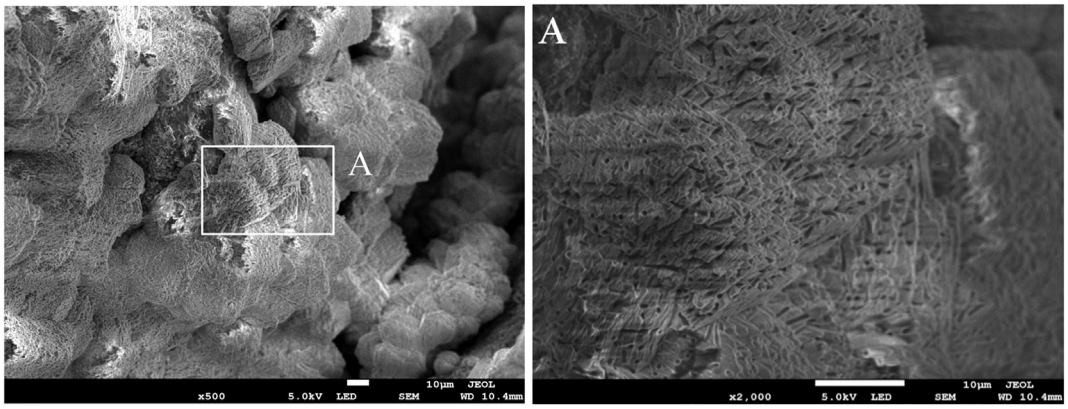

Fig. 7. Amorphous calcium carbonate (a) showing (b) traces of microorganisms on its surface.

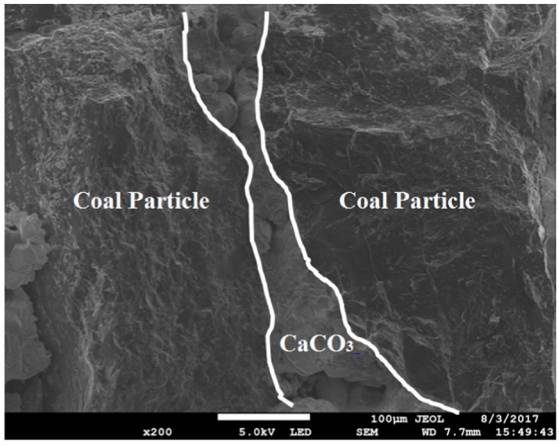

Fig. 9. Face to face bonding.

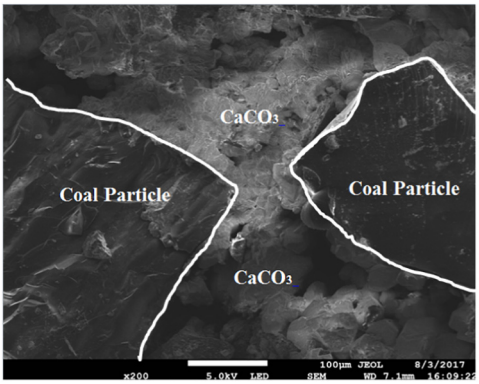

Fig. 10. Point to point bonding.

4 cycles of injection the maximum UCS (11.9 MPa) is for the 40–60 mesh sample although, its calcium carbonate content is not the highest. In contrast, the 20–40 mesh sample has the highest calcium carbonate content but the lowest UCS. This apparent anomaly is resolved if we examine the microscopic form of the cementation within the samples, following.

4. Microscopic phenomenon

We examine the role of the distribution of cementation within the sample to resolve the apparent contradiction between cementing mass and strength. Scanning electron microscopy (SEM) is used to analyze the microstructure of the deposited calcium carbonate and its distribution within the interparticle space.

4.1. Characteristics of microbial calcium carbonate

The SEM identifies overlapping hexahedral crystals [Fig. 6] with some surrounded by amorphous calcium carbonate [Fig. 7(a)]. During crystallization, the bacteria act as nuclei and are gradually surrounded. This impedes the transmission of nutrient ultimately rendering the bacterium inactive. Holes on the surface of the calcium carbonate represent traces left by the bacteria [Fig. 7(b)], identifying the role of microorganisms in the mineralization.

4.2. Microscale textures of calcium carbonate mineralization

Microorganisms first concentrate on the surface of the coal particles [Fig. 8] where they gradually generate calcium carbonate. As this mass increases, the particle is partially enveloped in calcium carbonate and the particles ultimately connected. As the void occludes, the cementation process slows, halts, as bacteria and nutrient are expended, and further supply is limited. Therefore, for a fixed duration of supply, the carbonate content of the lower-permeability small particle-size samples will be lower than that for larger particles. Although larger particle size samples can accommodate larger masses of calcium carbonate in a given time, the mass needed to cement two contacting particles also increases. This explanation is consistent with the observation that samples with larger particles have both a higher calcium carbonate content but a lower uniaxial compressive strength. In addition, it should be noted that the distribution of calcium carbonate on the coal surface is not uniform and the coal particles are not completely enveloped by the precipitation. This ensures that fluid transport is maintained and the main goal is of enabling hydraulic fracturing to reduce the drainage lengthscale by accessing the interior of the coalbed reservoir.

The individual coal particles are not spherical, resulting in cementation between particles taking two forms: face to face [Fig. 9] and point to point [Fig. 10] bonding. The former has a larger effective area of cementation and higher cemented strength.

5. Conclusions

A method of enhancing structural integrity and mechanical strength of mylonitized soft-coal reservoir has been proposed by microbially-induced calcium carbonate cementation. After 4 cycles of microbial injection, the maximum UCS reaches 11.9 MPa and the brittleness index of the coal samples approach or even exceed that of hard coal – suggesting susceptibility to hydraulic fracturing. However, a higher calcium carbonate content does not automatically guarantee a higher strength, with this mainly related to the architecture of the interparticle space.

SEM results show that the shape of microbially generated calcium carbonate cements is mainly hexahedral and some of crystals are surrounded by amorphous calcium carbonate. The cementation process for calcium carbonate is via interparticle bonding. Precipitation occurs first on the sample surfaces, partially enveloping them, before creating particle-particle bonds. Two forms of microbial cementation between particles include face to face bonding and point to point bonding.

This study indicates the potential to develop increased brittleness and improved compressive strength in coals, with the former index suggesting that the improvements are sufficient to allow successful hydraulic fracturing. The strengthening and embrittlement is significantly sensitive to subtle features of the nutrient penetration, distribution and resulting cementation architecture. This suggests that permeability and its heterogeneity are key features in enabling uniform sweep of injected fluids and the related delivery of nutrients that ultimately definine the potential for cementing and embrittling the coal and enabling its hydraulic fracturing.

Acknowledgments

This paper is supported by the National Science Foundation of China (No. 51604051), Natural Science Foundation of Chongqing (No. cstc2018jcyjA2664), China Scholarship Council (No. 201708500037), the National and Local Joint Engineering Laboratory of Traffic Civil Engineering Material of Chongqing Jiaotong University, the Chongqing Key Laboratory of Mountainous Road Structure and Material, and the Hi-tech Laboratory for Mountain Road Construction and Maintenance.

References

Achal, V., Pan, X., Zhang, D., 2011. Remediation of copper-contaminated soil by Kocuria flava CR1, based on microbially induced calcite precipitation [J]. Ecol. Eng. 37 (10), 1601–1605.

Bang, S.S., Galinat, J.K., Ramakrishnan, V., 2001. Calcite precipitation induced by polyurethane immobilized Bacillus pasteurii [J]. Enzym. Microb. Technol. 28 (s4–5), 404–409.

Benini, S., Rypniewski, W.R., Wilson, K.S., et al., 1999. A new proposal for urease mechanism based on the crystal structures of the native and inhibited enzyme from Bacillus pasteurii : why urea hydrolysis costs two nickels [J]. Structure 7 (2), 205–216.

Brittleness index[M]. Springer, Berlin Heidelberg.

Chun, L., 2014. Study on Mechanism and Controlling of Borehole Collapse in Soft Coal Seam.

Dejong, J.T., Fritzges, M.B., Nüsslein, K., 2006. Microbially induced cementation to control sand response to undrained shear[J]. J. Geotech. Geoenviron. Eng. 132 (11), 1381–1392.

Dejong, J.T., Mortensen, B.M., Martinez, B.C., et al., 2010. Bio-mediated soil improvement[J]. Ecol. Eng. 36 (2), 197–210.

Hajiabdolmajid, V., Kaiser, P., 2002. Brittleness of rock and stability assessment in hard rock tunneling[J]. Tunnelling Undergr. Space Technol. Incorp. Trenchl. Technol. Res. 18 (1), 35–48.

Hucka, V., Das, B., 1974. Brittleness determination of rocks by different methods[J]. Int. J. Rock Mech. Min. Sci. Geomech. Abstr. 11 (10), 389–392.

Jabri, E., Carr, M.B., Hausinger, R.P., et al., 1995. The crystal structure of urease from Klebsiella aerogenes.[J]. Science 268 (5213), 998–1004.

Kaltwasser, H., Kramer, J., Conger, W.R., 1972. Control of urease formation in certain aerobic bacteria [J]. Arch. Microbiol. 81, 178–196.

Meng, F., Zhou, H., Zhang, C., et al., 2015. Evaluation methodology of brittleness of rock based on post-peak stress–strain curves[J]. Rock Mech. Rock. Eng. 48 (5), 1787–1805.

Mobley, H.L., Hausinger, R.P., 1989. Microbial ureases: significance, regulation, and molecular characterization [J]. Microbiol. Rev. 53 (1), 85–108.

Paassen, L.A.V., 2009. Biogrout, Ground Improvement by Microbial Induced Carbonate Precipitation [D].

Wang, G., Li, W., Wang, P., et al., 2017a. Deformation and gas flow characteristics of coal-like materials under triaxial stress conditions [J]. Int. J. Rock Mech. Min. Sci. 91, 72–80.

Wang, G., Wu, M., Wang, R., et al., 2017b. Height of the mining-induced fractured zone above a coal face [J]. Eng. Geol. 216, 140–152.

Xia, Y.J., Li, L.C., Tang, C.A., et al., 2017. A new method to evaluate rock mass brittleness based on stress–strain curves of class I[J]. Rock Mech. Rock. Eng. 50 (5), 1–17.

Zhang, S., Su, X., Guo, H., et al., 2014. Controlling the damage of conductivity of hydraulic fractures during the process of drainage in coalbed methane well [J]. J. China Coal Soc. 39 (1), 124–128.

Zhang, D., Ranjith, P.G., Perera, M.S.A., 2016. The brittleness indices used in rock mechanics and their application in shale hydraulic fracturing: a review [J]. J. Pet. Sci. Eng. 143, 158–170.

Zou, Y., Ma, X., Wang, L., et al., 2011. Experimental evaluation of conductivity of fracturing in medium and high-rank coalbed [J]. J. China Coal Soc. 36 (3), 473–476.